Superlattices and Microstructures, Vol. 25, No. 1/2, 1999
Article No. spmi.1998.0647
Available online at http://www.idealibrary.com on IDEAL

Experimental demonstration of electron switching in a quantum-dot cellular automata (QCA) cell

ISLAMSHAH AMLANI†, ALEXEI O. ORLOV, GREGORY L. SNIDER,
CRAIG S. LENT, WOLFGANG POROD, GARY H. BERNSTEIN
Department of Electrical Engineering, University of Notre Dame, Notre Dame, IN 46556, U.S.A.

(Received 26 October 1998)

We present an experimental demonstration of electron switching in a quantum-dot cellular automata (QCA) cell. The four-dot QCA cell is constructed of two capacitively-coupled double-dots. Polarization switching of the cell is accomplished by applying biases to the gates of the input double-dot and is experimentally verified from the conductances of electrometers capacitively coupled to the output double-dot. Theoretical simulations of the QCA switching show excellent agreement with experiment. We include preliminary results of a modified cell design that show improved performance.

Key words: nanodevices, quantum devices, singl electronics, tunneling.

1. Introduction

Quantum-dot cellular automata (QCA) architecture [1–3] is a transistorless computation paradigm that uses nanometer-scale dots. In contrast to the existing digital technology in which logic levels are encoded as voltages on capacitors, the information in this new paradigm is encoded in the positions of the electrons within the dots. QCA can be realized in any material system where dot barriers are sufficiently high and dot capacitances are sufficiently small ensuring quantization of charge on the dots due to the Coulomb blockade of electron tunneling [4].

A basic QCA cell can be visualized as a coupled-dot system with four dots positioned at the corners of a square (Fig. 1A). If the cell is charged with two excess electrons, they will occupy diagonal sites within the cell due to electrostatic repulsion (Fig. 1B). The two possible arrangements, being energetically equivalent, are the ground states of the cell. These two polarization states can be used to represent stable states of digital logic. All Boolean logic functions can be realized by an appropriate arrangement of these basic cells.

In this paper, we will consider two different designs of a QCA cell. Figure 1C shows the first version of our QCA cells which is formed by two, capacitively-coupled double-dots. Polarization switching in the cell is produced by applying input gate biases. If each double-dot is biased to contain an extra electron, switching of an electron in the input double-dot will induce an opposite electron switch in the output double-dot culminating in a polarization switch of the cell. The switching can be experimentally observed by tracking the position of electrons in each double-dot. There are two ways to verify an electron exchange in a double-dot. The first way

†E-mail: Islamshah.amlani.1@nd.edu

0749–6036/99/010273 + 06 $30.00/0

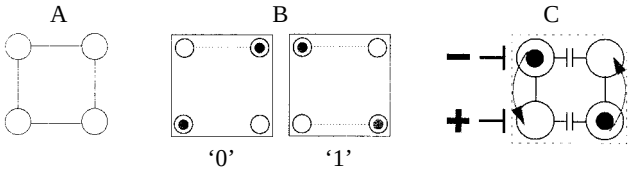

Fig. 1. Description of the QCA cell used in our study. A, Basic QCA cell. B, Two possible polarizations of the cell. C, Electron switching in the QCA cell under the influence of applied input bias.

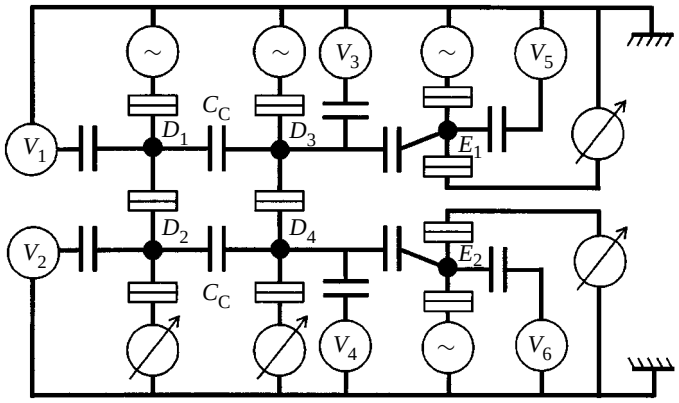

Fig. 2. Schematic diagram of the six-dot QCA system.

is to measure the conductance through a double-dot as a function of predetermined input gate voltages. An alternate way is to use single-electron tunneling transistors (SET) as electrometers [5]. If properly calibrated, electrometers can noninvasively measure potential variations of a double-dot [6]. We use the former technique to control and observe the switching in the input double-dot and the latter technique to externally detect the opposite switching in the output double-dot.

2. Fabrication and measurement

Figure 2 shows the schematic diagram of our six-dot QCA system using tunnel-junction notation. We will refer to the input and output double-dots as D_1D_2 and D_3D_4, respectively. Each dot of the cell is capacitively coupled to a gate electrode. Dots D_3 and D_4 are also capacitively coupled to electrometers labeled E_1 and E_2, respectively. Electrostatic coupling between D_1D_2 and D_3D_4 is provided by capacitors labeled C_C. Later, we will briefly discuss our modified version in which these coupling capacitors are replaced by a tunnel junction.

Fabrication of metal-tunnel junctions is accomplished using electron beam lithography and a double-angle, shadow evaporation technique [7]. Tunnel junctions are formed by oxidizing the first layer of Al *in situ* prior to depositing the second layer. All measurements are performed in a dilution refrigerator. Conductances of the double-dots and electrometers are measured using standard lock-in techniques with an excitation voltage of 4 μV at 16–40 Hz. A magnetic field of 1 T is applied to suppress the superconductivity of the Al metal. Junction capacitances are extracted from the charging energies of the electrometer dots. Other gate and capacitance-coupling parameters are determined from the period of the Coulomb blockade oscillations.

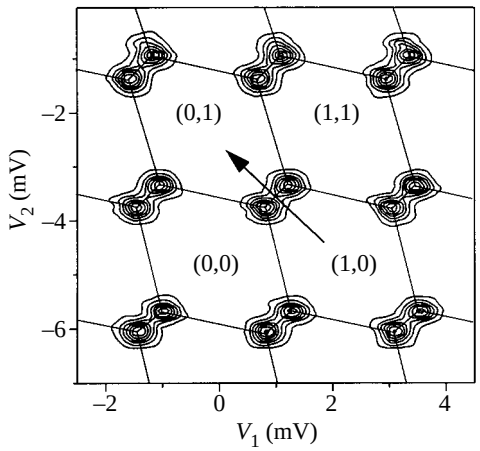

Fig. 3. Charging diagram of the input double-dot as a function of the gate voltages V_1 and V_2. Charge configurations (n_1, n_2), which represent the number of extra electrons on D_1 and D_2, respectively, are arbitrarily chosen.

3. Results and discussions

Figure 3 shows a contour plot of conductance through D_1D_2 as a function of V_1 and V_2. This plot, referred to as the charging diagram, can be used to map out the occupancy phase diagram for the double-dot system (the charging diagram for D_3D_4 is similar) [8]. Each conductance peak splits due to the interdot capacitive coupling provided by the tunnel junction. Note the non-zero conductance due to finite thermal energy around the split peak, forming a 'saddle point' between the peaks. Solid lines have been added that connect these conductance peaks to delineate the boundaries between the fixed charge regions (n_1,n_2), where n_1 and n_2 represent the excess dot populations of D_1 and D_2, respectively. In the interior of each hexagonal cell, charge configurations of the double-dot are fixed. If the gates are scanned in the direction of the arrow, the charge configuration will change from (1,0) to (0,1), representing an electron switch in the double-dot. We will refer to this scan direction as the input diagonal voltage. The conductance peak at the saddle point as a function of the input diagonal voltage can be used as a marker between the charge states (1,0) and (0,1).

As an electron switches from D_1 to D_2 under the influence of the applied gate bias, each dot undergoes an abrupt potential change due to the addition or removal of an electron. If the gates are scanned in the direction indicated in Fig. 3, D_1 will lose an electron resulting in a positive potential shift and D_2 will gain an electron resulting in a negative potential shift. These potential shifts act as extra gate voltages to the capacitively-coupled D_3D_4 and are reflected as a sharp displacement in the charging diagram of D_3D_4 along the charge exchange direction. The magnitude of this displacement depends on the coupling capacitances C_C, and the amplitude of the potential shifts produced by an electron switch in D_1D_2. If D_3D_4 is initially biased in the vicinity of the saddle point by V_3 and V_4, the sharp displacement induced by D_1D_2 will shift the saddle point from one side of the bias point to another, resulting in a polarization change of D_3D_4. It must be emphasized that the role of V_3 and V_4 is only to bias D_3D_4 near the saddle point; the polarization change is solely due to the potential shifts induced by D_1D_2.

We measure the conductances of the electrometers simultaneously as a function of the input diagonal voltage to experimentally verify the electron exchange in D_3D_4. Both electrometers are biased on the positive slope of a conductance peak to ensure an identical response. Figure 4A shows the conductance of D_1D_2 indicating an electron hop from D_1 to D_2. The peak in the conductance occurs at the saddle point between the charge states (1,0) and (0,1). Coincident with an electron switch in D_1D_2, we see a sharp change in the conductance of each electrometer. A downward shift in the conductance of E_1 represents addition of an electron on D_3.

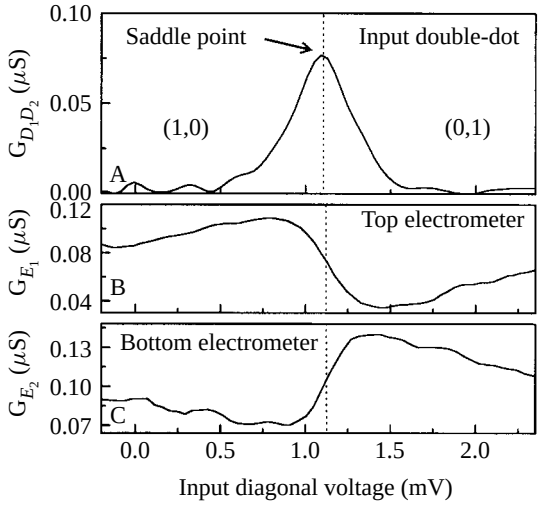

Fig. 4. A, Conductance through the input double-dot as a function of the diagonal voltage (Fig. 3). The peak indicates the switch of an electron from D_1 to D_2. B, Conductance through E_1 indicating the addition of an electron to D_3, and C, through E_2 indicating the removal of an electron from D_4.

Similarly, an upward shift in the conductance of E_2 represents removal of an electron from D_4. Hence, the data in Fig. 4 show a controlled polarization change of the QCA cell.

We use classical Coulomb blockade theory to simulate the potentials and charges on each dot of the QCA cell during the polarization change. A matrix of all capacitances is included in the calculations and finite temperature effects are incorporated by performing thermodynamic averaging over all accessible charge configurations. In the simulation, background charge and temperature are the only parameters used to fit the measured data. Background charge only shifts the position of the peaks and does not change the amplitude or the period of the potential swing. Figure 5A shows the experimental and theoretical curves of potential on D_3 during the switching. As can be seen, the experimental results are in excellent agreement with the theoretical predictions. The results are calculated for $T = 75$ mK which is in close agreement with the actual device temperature. Figure 5B shows the calculated charges on dots D_3 and D_4 during the charge exchange. At the temperature of the experiment, an electron switch in D_1D_2 causes approximately 70% polarization change in D_3D_4.

In order to improve the polarization change of D_3D_4, we have made some modifications to the previous design. The new version appears in Fig. 6A where we have replaced the coupling capacitors of the previous design (Fig. 3) by a tunnel junction. This would result in a stronger electrostatic coupling between D_1D_2 and D_3D_4 considering that the tunnel junctions exhibit the most dominant capacitances in our device. Larger coupling capacitance between D_1D_2 and D_3D_4 is desired, as it will increase the shift of the charging diagram for D_3D_4, due to potential swings of D_1D_2. As seen in Fig. 5B, the finite temperature smears out the transition region resulting in a polarization change of only 70% in D_3D_4. If the shift in the charging diagram of D_3D_4 can be made larger to accommodate the width of the temperature smearing, a polarization change of 100% can be achieved.

We present preliminary results of our new device using the same theoretical model used to fit the data in the previous experiment. In the calculations, we use the measured junction and gate capacitances to compute the dot charges for D_3 and D_4. The simulated curves are shown in Fig. 6B. As can be seen, the predicted polarization change in D_3D_4 using the modified design is almost 100%.

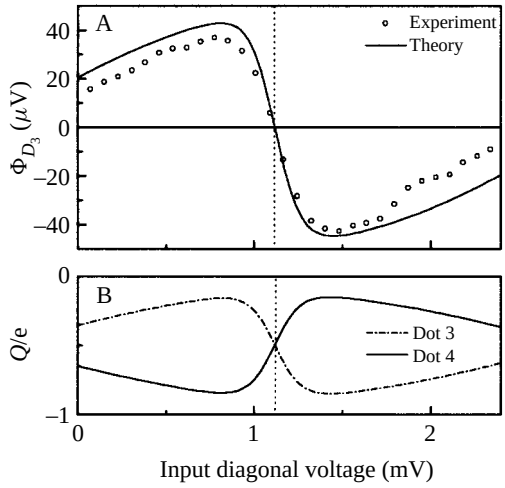

Fig. 5. A, Experimental and theoretical curves showing potential change on dot D_3 as a function of the input diagonal voltage. The solid line represents the simulation result at 75 mK, and the dotted line shows the experimental values calculated from the conductance of E_1. B, Theoretical calculations of the charges on dots D_3 and D_4 during QCA polarization change.

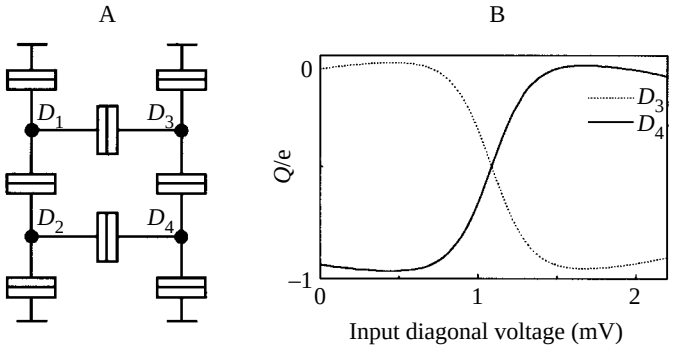

Fig. 6. A, Schematic diagram of the modified version of the QCA cell. B, Theoretical calculations of the charges on dots D_3 and D_4 during QCA polarization change. Results are computed using the measured capacitances of the QCA cell in Fig. 6A.

4. Conclusions

We have used Coulomb blockade effects to demonstrate polarization change in a four-dot QCA cell. Switching in the cell is induced by applying input gate voltages and verified from the electrometer signals. Agreement between the theoretical predictions and the experimental result is excellent. Theoretical simulations using the actual capacitances of the modified cell design show more promising results with almost 100% polarization change of the cell.

Acknowledgements—This research was supported in part by DARPA, ONR (grant number N0014-95-1-1166) and NSF. We wish to thank J. Merz for helpful discussions.

References

[1] C. S. Lent, P. D. Tougaw, and W. Porod, Appl. Phys. Lett. **62**, 714 (1993).
[2] C. S. Lent, P. D. Tougaw, W. Porod, and G. H. Bernstein, Nanotechnology **4**, 49 (1993).

[3] C. S. Lent and P. D. Tougaw, Proc. IEEE **85**, 541 (1997).
[4] G. L. Ingold and Yu. V. Navarov, *Single Charge Tunneling*, edited by H. Grabert and M. H. Devoret, (Plenum, New York, 1992) Chap. 2.
[5] P. Lafarge, H. Pothier, E. R. Williams, D. Esteve, C. Urbina, and M. H. Devoret, Z. Phys. **B85**, 327 (1991).
[6] I. Amlani, A. O. Orlov, C. S. Lent, G. L. Snider, and G. H. Bernstein, Appl. Phys. Lett. **71**, 1730 (1997).
[7] T. A. Fulton and G. H. Dolan, Phys. Rev. Lett. **58**, 109 (1987).
[8] H. Pothier, P. Lafarge, C. Urbina, D. Esteve, and M. H. Devoret, Europhys. Lett. **17**, 249 (1992).